Effects of deformation on neutron total cross sections of even-A Nd and Sm isotopes

R. E. Shamu, E. M. Bernstein, and J. J. Ramirez*
Western Michigan University, Kalamazoo, Michigan 49008

Ch. Lagrange
Centre d'Etudes de Bruyères-le-Châtel, 92542 Montrouge Cedex, France

(Received 4 June 1980)

Neutron total cross sections of ^{144}Nd and ^{148}Sm and total cross-section differences for the pairs of isotopes ^{144,142}Nd, ^{146,144}Nd, ^{148,144}Nd, ^{150,144}Nd, ^{150,148}Sm, ^{152,148}Sm, and ^{154,148}Sm have been measured at 25 energies from 0.75 to 14 MeV. Each sample consisted of about 40 g of powdered oxide with an isotopic enrichment $>94\%$. For each isotopic pair the total cross-section difference was determined directly by measuring the ratio of transmitted flux for matched samples. This difference was found to have an oscillatory behavior when plotted as a function of incident neutron energy. The oscillations have been explained as a deformation effect *qualitatively* in terms of the nuclear Ramsauer effect and *quantitatively* using a deformed optical model potential. Adding two neutrons to a nucleus in this mass region was found to have a different effect on the neutron total cross section than adding two protons. A coupled channel analysis was performed using as input data the present total cross sections, low-energy neutron scattering parameters, and elastic and inelastic (2^+) differential cross sections for neutron scattering at 4 and 7 MeV. Excellent total cross-section fits were obtained for the Sm isotopes; however, the total cross-section fits for the Nd isotopes were only fair. Quadrupole deformation parameters have been deduced for all the isotopes studied. The sensitivity of neutron total cross-section differences to this parameter and to the real isospin term of the nuclear potential is discussed.

[NUCLEAR REACTIONS ^{142,144,146,148,150}Nd, $E_n = 0.75$–13.89 MeV, ^{148,150,152,154}Sm, $E_n = 0.75$–14.49 MeV; measured $\sigma_{n,\mathrm{tot}}(E)$. Enriched targets. Deduced coupled-channel optical-potential parameters, quadrupole deformation parameters.]

I. INTRODUCTION

Nuclear deformations may be determined experimentally either by studying the nuclear charge distribution, that is, the distribution of protons, or the nuclear mass distribution, i.e., the distribution of neutrons plus protons. Since there is no reason to believe *a priori* that the charge and mass distributions of nuclei are identical, it is important to determine both of them. Recent experimental and theoretical developments have stimulated numerous studies of nuclear deformation during the last few years.[1]

Detailed information can be obtained about the shape of the proton distribution of nuclei from electron scattering studes,[1,2] for example, because the electromagnetic interaction is well understood. However, mass deformation experiments are more difficult to interpret since these studies require hadronic probes. The results of these hadron experiments usually are interpreted in terms of a nuclear potential model.[3] Although the exact relationship between the nuclear potential and nuclear mass distribution is not clear at present,[4] recent advances in Hartree-Fock theory[5] suggest that the solution to this problem may be forthcoming.

Neutrons are excellent probes for studying the deformation of the nuclear potential because the electromagnetic effects which complicate the analyses of charged hadron experiments, e.g., Coulomb excitation, are not present. Furthermore, the effects of nuclear deformation on neutron scattering are substantial over a wide range of energies. It has been known for many years that certain low-energy neutron scattering parameters, e.g., the s-wave strength function, have a strong dependence on nuclear deformation.[6] More recently, total cross section measurements[7] and differential cross section measurements[8,9] on the Sm isotopes have demonstrated that deformation effects are large for neutrons with energies in the MeV range. Neutron experiments utilizing an oriented ^{165}Ho target[10] suggest that these effects may be significant up to 100 MeV.

It should be emphasized that different experiments, even with the *same* probe, may not measure the same deformation. For a rotational nucleus, for example, neutron elastic scattering is sensitive only to the shape of the ground state, whereas neutron inelastic scattering depends, also, on the shapes of one or more excited states. The ground and excited states have the

same shape only in the limit that the nucleus in question is a rigid rotator. Since the *total* cross section is the sum of all the partial cross sections, it is not obvious on what shape this cross section depends. This question has been answered by Soga, who has shown that the total cross section, similar to the elastic scattering cross section, is sensitive only to the ground state deformation (see Appendix).[11]

In the present work, neutron total cross sections for ^{144}Nd and ^{148}Sm, and total cross section differences for ^{144,142}Nd, ^{146,144}Nd, ^{148,144}Nd, ^{150,144}Nd, ^{150,148}Sm, ^{152,148}Sm, and ^{154,148}Sm have been measured from 0.8 to 14 MeV. These Nd and Sm isotopes are particularly desirable nuclei for studying nuclear deformation since they span the region near $N = 88$ where the magnitude of the deformation and the type of collective motion[12] change dramatically for a small change in A. The isotope ^{142}Nd, with a closed neutron shell, is an excellent example of a vibrational nucleus, whereas ^{154}Sm, with many neutrons and protons outside closed shells, is believed to be a rigid rotator.[12] (We have chosen to compare the Nd isotopes to ^{144}Nd rather than singly magic ^{142}Nd for a number of reasons, as discussed in Sec. II B.) The quadrupole deformation parameter of the nuclear potential was determined for each isotope studied by means of a coupled-channel analysis.[13-15]

The effect of nuclear deformation on neutron total cross sections was first measured at 0.35 MeV for an *oriented* target, ^{165}Ho.[16] Later total cross section measurements from 2.5 to 15 MeV on nuclei over a broad range of masses, when compared with spherical optical model calculations, indicated that deformation effects were also appreciable for *unoriented* targets.[17] A study of the separated isotopes ^{150,152,154}Sm from 0.8 to 15 MeV neutron energy[7] demonstrated that deformation effects were evident in total cross section differences, had a strong dependence on incident energy, and could be as large as 10%. The interpretation of each of these various observations as a nuclear potential deformation effect was supported by coupled-channel optical model calculations.[7,14,16,18]

Total cross sections have been measured previously for ^{144,146,148}Nd and ^{152}Sm at low neutron energies by Pineo *et al.*[19] and for all the separated isotopes studied in the present work at 14.2 MeV by Dyumin *et al.*[20]

The experimental details of the present study are given in Sec. II. The coupled-channel optical model calculations employed to interpret the data are described in Sec. III. The measured cross sections and calculated values are presented in Sec. IV and discussed in Sec. V. Finally, Sec. VI is a statement of the conclusions of the present work. Preliminary reports of portions of this work have been given previously.[21,22]

II. EXPERIMENTAL DETAILS

A. Samples

The rare earth samples were obtained on loan from the Department of Energy in the form of isotopically enriched powdered oxides.[23] The experiments were performed with these samples in oxide form since the cost of converting them to metallic form was prohibitive. The isotopic composition of each sample is given in Table I. The total metallic impurity content of each sample was less than 2 atomic percent. Water (and possibly CO_2) was driven from each oxide by heating it in a ceramic crucible at 800 °C for about 16 h and then allowing it to cool in a desiccator.

After cooling, the dry oxide was transferred to a vacuum-tight sample container. The oxide was vibrated and compressed in the container during the transfer to avoid the formation of large voids. An estimate of the mass of water adsorbed during transfer was made by determining the oxide mass before and after transfer. Except for the $^{142}Nd_2O_3$ sample, each oxide was estimated to gain (10 ± 5) mg during transfer. This estimate was checked by drying and packing some of the oxides several times. Because the $^{142}Nd_2O_3$ powder tended to adhere strongly to the tools employed, its transfer took much longer and, also, the mass of adsorbed water could not be estimated as precisely. The mass of adsorbed water for this oxide was estimated to be (60 ± 30) mg.

The sample containers were thin-walled stainless steel cells 1.4 cm in diameter and about 15 cm long. One end of each cell was closed by a stainless steel cap which was hard-soldered in place and the other end by an adjustable cap sealed with an O-ring. The adjustable cap permitted a predetermined mass of oxide to be used for each sample along with the condition that the ends of the powdered sample remained flat and parallel. The flat parts of the fixed and adjustable caps were about equal in thickness and were matched so that for each cell the total thickness of the two end caps was (0.97 ± 0.03) mm. The mass of each of the rare earth oxide samples used is given in Table I. For each element the number of nuclei was the same for all the isotopes to within 0.1%. The areal densities were 0.0943 Nd atoms/b and 0.0959 Sm atoms/b for the Nd and Sm samples, respectively.

The oxygen contribution to the $^{144}Nd_2O_3$ and $^{148}Sm_2O_3$ cross sections was determined using a BeO sample in the form of a powder[24] and a Be

TABLE I. Isotopic compositions and masses of the Nd_2O_3 and Sm_2O_3 samples.

Element	Sample	Isotopic composition (at.%) 142	143	144	145	146	147	148	149	150	152	154	Oxide mass (g)
							%Nd						
Nd	142	96.24	2.06	0.99	0.24	0.33		0.08		0.06			37.38
	144	1.31	1.66	94.50	1.47	0.88		0.11		0.07			37.80
	146	0.43	0.20	0.70	0.69	97.46		0.32		0.13			38.24
	148	1.14	0.56	1.18	0.58	1.76		94.07		0.79			38.70
	150	0.77	0.39	0.88	0.34	0.84		0.66		96.13			39.12
							%Sm						
Sm	148			0.04			1.30	96.40	1.46	0.25	0.37	0.20	39.38
	150			0.05			0.39	0.47	1.70	95.48	1.46	0.45	39.82
	152			0.02			0.20	0.19	0.29	0.24	98.29	0.76	40.26
	154			0.02			0.14	0.12	0.17	0.12	0.74	98.69	40.76

sample[25] consisting of a machined cylinder of metallic Be. The areal density of each of these two samples was 0.2319 molecules/b, which is larger than the value required for a direct subtraction of the effect of oxygen. A larger value was chosen so that a precise measurement of the oxygen cross section could be performed easily. This measurement served as a check on our experimental procedure at a number of energies. The difference in areal density between the rare earth samples and Be-BeO samples was, of course, taken into account in computing the ^{144}Nd and ^{148}Sm total cross sections.

The experimental procedure was also tested by measuring the n-p total cross section. Samples of polyethylene and reactor-grade graphite were employed for these checks. The Be, BeO, C, and polyethylene samples all were placed in containers essentially identical to those of the rare earth oxides.

B. Method

Measurements were performed at 27 neutron energies over the range 0.75 to 14.5 MeV using monoenergetic neutrons from the ^{3}H(p,n) reaction at 5.0 MeV and lower energies, and from the ^{2}H(d,n) reaction at 4.5 MeV and higher energies. The protons or deuterons were accelerated by the Western Michigan University HVEC model EN tandem accelerator. The tritium was contained in a 1.2 mg/cm^2 layer of Ti evaporated onto a 0.25 mm Pt backing.[26] The neutron energy spread for this target was measured to be 94±2 keV at 2.078 MeV neutron energy by determining both the width and the apparent shift of the sharp carbon resonance at that energy.[27] The target thickness thus determined corresponds to a neutron energy spread ranging from 140 keV at 0.75 MeV energy to 56 keV at 5.0 MeV. The deuterium was contained in either a 2-cm long or 4-cm long gas target by a 1.2 μm Ni entrance foil. The foil thickness was determined by measuring the energy loss through the foil of 5.486 MeV alpha particles from a ^{241}Am source. The gas pressure was adjusted so that the neutron energy spread was less than 70 keV, except at 5.47 and 6.25 MeV, where it was 100 and 80 keV, respectively. Since the energy of the incident protons or deuterons had an uncertainty of less than 5 keV,[28] it is believed that the uncertainty in energy of the neutrons was 10 keV or less over the energy range investigated. The neutron flux was monitored by a long counter placed at 60° with respect to the incident proton or deuteron beam.

The neutrons were detected with a stilbene scintillator 1.9 cm in diameter and 2.5 cm long mounted on an RCA 8575 photomultiplier tube. The scintillator was 50 cm from the neutron-producing target and at 0° with respect to the incident protons or deutrons. Pulses from γ rays were eliminated using the ORTEC pulse-shape discrimination system. A time spectrum from this system for 3.6 MeV incident neutrons is shown in Fig. 1. The separation of the two peaks decreased slowly with increasing neutron energy; however, this effect was accompanied by a narrowing of the neutron peak. As a consequence, the ratio between the height of the neutron peak and the valley between peaks was sufficient for good n-γ separation except at 0.75 MeV. At this energy it was necessary to bias up on the high channel side of the neutron peak to eliminate γ-ray counts. At 0.75 MeV as well as at other neutron energies the shape of the γ-ray peak was studied over a wide γ-ray energy range using a variety of sources. These tests indicated that the number of γ rays counted was negligible at each of the neutron energies of

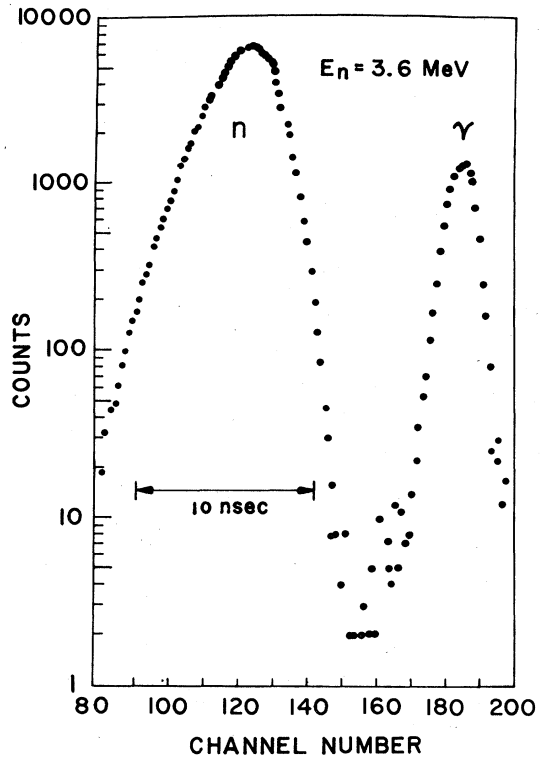

FIG. 1. Time spectrum from the neutron-gamma pulse-shape discrimination system at E_n=3.6 MeV.

the present work.

It was necessary to place the samples at one-third of the distance from the neutron-producing target to the detector, instead of the usual half-way point,[29] in order to completely shadow the scintillator cell. The additional inscattering caused by this particular placement was not appreciable.

Separate sets of measurements were made on the Sm isotopes[21] and on the Nd isotopes[22] with an interval of about six months between the two experiments. Procedures were essentially identical for both studies. The isotope ^{150}Sm, which was included also in the Nd study, served as a check on the consistency of the two experiments (see Sec. IIC).

For each element two types of measurements were performed at each energy: the total cross section of an isotope believed to have a relatively small deformability (^{144}Nd for Nd and ^{148}Sm for Sm) and the total cross section *difference* between this isotope and each of the other isotopes of that element. The nucleus ^{144}Nd was chosen for Nd rather than singly magic ^{142}Nd because the ^{144}Nd sample was superior (see Sec. IIA) and because ^{144}Nd and ^{148}Sm have very similar values of the asymmetry parameter $(N-Z)/A$. The ^{144}Nd and ^{148}Sm total cross sections were measured in the standard way using as samples $^{144}Nd_2O_3$ or $^{148}Sm_2O_3$, BeO, Be, and a blank can. The total cross section difference, e.g., between ^{146}Nd and ^{144}Nd, was determined *directly* by measuring the transmission ratio for the oxides of these two isotopes. Determining the difference directly from this ratio has several important advantages over subtracting two independent cross-section determinations: (1) the effects of the containers and of the oxygen in the two samples cancel, and (2) most of the systematic errors of the transmission measurement essentially cancel, as explained in Sec. IV.

Whenever it was possible, data were taken at a neutron energy for which the oxygen total cross section was at a local minimum. For each of these cases the energy at the minimum was determined experimentally by measuring the transmission of the BeO sample over a small neutron energy range. The energies of these minima are in good agreement with the total cross section data of Schwartz *et al.*[30]

C. Procedure

For each element, measurements were made at each neutron energy in a series of about 30 runs. The duration of each run was fixed by integrating the beam current to a predetermined total charge. The beam current was adjusted to 0.5 μA or less at each energy in order to keep count rate effects for each of the measured transmissions below 0.3%. At higher energies, beam currents were kept below 0.15 μA to reduce pileup in the pulse-shape discrimination system.

The runs were ordered so that effects caused by slow drifts in the neutron flux and in the electronic systems were minimized; e.g., the sample sequence 154, 148, 152, 152, 148, 154 was employed for the ^{154,148}Sm and ^{152,148}Sm differences. Two linear biases were set on the proton recoil distribution from the stilbene scintillation (usually at $\frac{1}{2}$ and $\frac{3}{4}$ of the pulse height corresponding to the maximum-energy recoil) in order to check the gain stability of the detection system. The lower bias was increased for the higher energy data so that break-up neutrons would not be counted.

Beam-associated background was measured either by using a blank ^{3}H-Ti target or by evacuating the gas target. Background from room-scattered neutrons was determined using a copper shadow cone. Each of these backgrounds was always less than 2% of the sample-out neutron flux.

The energy range of interest was covered as follows. For the ^{2}H(d,n) source reaction and the Sm isotopes, for example, the experiment was

initiated at 5.00 MeV neutron energy with a measurement of the n-p total cross section to a statistical uncertainty of about 0.5%. Data then were taken in steps of about 1 MeV up to the maximum energy, 14.5 MeV. The energies selected going down from this maximum energy generally were interleaved between those chosen going up. Only minor adjustments were made to the pulse-shape discrimination system in proceeding from one energy to the next one. Similar procedures, that is, an n-p check at 5.00 MeV and interleaving energies, were followed when covering the neutron energy range 5.00 to 0.75 MeV with the ^{3}H(p,n) source reaction.

The stability of the beam-current integration system could be monitored with precision by the long counter only up to about 12 MeV neutron energy. Above this energy, the beam-associated background detected by the long counter (mostly from the gold beam stop) was substantial. The performance of the integration system over the energy range which could be monitored, 0.75 to 12 MeV, indicated that its operation was reliable within the statistical accuracy of the monitor, which was generally smaller than 0.3%.

Corrections were made to each of the measured transmissions for beam-associated background and background from room-scattered neutrons. The ^{144}Nd and ^{148}Sm total cross section data were corrected for single inscattering. For the $^{144}Nd_2O_3$ sample, for example, the inscattering correction to the transmission ranged from 0.3% at 0.75 MeV to 1.0% at 14 MeV. The effect of inscattering on the cross section *difference* data was very small, hence no such correction was made to these data.

The ^{144}Nd and ^{148}Sm total cross sections were also corrected for the presence of 10 mg of water which was adsorbed by the oxides during the filling of their respective sample containers. This correction ranged from 0.4% of the measured cross section at 0.75 MeV to 0.1% at 15 MeV. The correction for the presence of water was not significant for the total cross section differences with the exception of the differences for ^{144,142}Nd. Because of the presence of 60 ± 30 mg of water in the $^{142}Nd_2O_3$ sample (see Sec. II A), the water correction for the relative difference $[\sigma(^{144}\text{Nd}) - \sigma(^{142}\text{Nd})]/\sigma(^{144}\text{Nd})$ was large, ranging from +0.023 at 0.75 MeV to +0.007 at 14 MeV.

A total of five determinations of the n-p total cross section at 5 MeV were made during the course of the Nd and Sm measurements. The weighted mean of these five values was 1.639 ± 0.004 b, which is in good agreement with the value of 1.635 b calculated by Hopkins and Breit from the Yale Y-IV phase shift set.[31] Total cross sections calculated from these phase shifts are in excellent agreement with n-p measurements from 1 to 25 MeV.[32] Relative differences between the individual determinations of the present work and the Hopkins-Breit value ranged from −1.2% to 1.3%.

The experimental procedure was checked at other energies by comparing the oxygen total cross sections of the present work with those of Schwartz *et al.*[30] at selected energies for which energy resolution effects were unimportant. The agreement was good over the entire energy range of the comparisons, 2.7 to 14.5 MeV.

Lastly, the value of the ^{150}Sm total cross section obtained at each energy in the Nd experiment was compared with the corresponding value from the Sm study to search for any systematic differences which might exist between the results of the two experiments. The Nd value was determined from the ^{144}Nd total cross section and the (^{150}Sm − ^{144}Nd) cross section difference, and the Sm value was computed from the ^{148}Sm total cross section and the (^{150}Sm − ^{148}Sm) cross section differences. At each energy the agreement between the two sets of data was consistent with the statistical uncertainties, which were 1.5% or less for each of the two experimental ^{150}Sm cross sections. Precise estimates of systematic differences between the two experiments were made by averaging cross sections over a number of consecutive energies, thus reducing the effect of statistical fluctuations. Average ^{150}Sm cross sections were computed for the ^{3}H(p,n) data ($E_n < 5$ MeV) and the ^{2}H(d,n) data ($E_n \geq 5$ MeV) for each of the two experiments. The averages were found to differ by (0.3 ± 0.4)% and (0.2 ± 0.5)% below and above 5 MeV, respectively.

III. COUPLED CHANNEL CALCULATIONS

The coupled-channel optical model utilized in the present work has been described in detail elsewhere,[9,15] therefore only a brief description will be given here. A fundamental assumption of the present analysis is: Provided that the contributions of the strong collective states to the optical potential are taken into account explicitly by means of coupled-channel calculations, the strength and geometric parameters of the resulting potential are valid over a broad mass range. This assumption is consistent with the formulation of nuclear reaction theory presented by Feshbach[33] and has been demonstrated to be valid for the scattering of 50 MeV alpha particles from nuclei in the rare earth region by Glendenning *et al.*[3] These authors found that the same potential could be used, with only minor adjustments, from the vibrational nucleus ^{148}Sm through the deformed region up to ^{178}Hf. Thus, for an analysis of a

sequence of isotopes which have various deformations, only the *shape* of the potential, i.e., the deformation parameters, must be changed from isotope to isotope. In the present analysis we have also varied the *strength* of the optical potential by including real and imaginary isospin terms, since such terms, although not present for alpha-particle scattering, are well established for nucleon-nucleus scattering.[34]

The set of neutron data included in the present analysis consisted of the following data on separated isotopes of Nd and Sm: (1) strength functions and potential scattering radii determined in the keV neutron energy region[19,35-37] (2) total cross sections and total cross section differences[19,21,22] from a few hundred keV to 15 MeV; and (3) elastic and inelastic differential cross sections at 4.08 MeV (Ref. 38) and at 7.0 MeV.[9,39] In addition, (p,p) and (p,p') data on the isotopes ^{148,152,154}Sm at 16 MeV (Ref. 40) were considered in order to define more precisely the magnitude of the isospin terms,[41] in particular, the imaginary part.

Except for the isospin terms, the interaction potential utilized in the present work was essentially that described by Tamura.[13] Thus, we have assumed

$$V(r,\theta,\phi) = -(V + iW_V)f(r,a,R) + iW_D 4a' \frac{d}{dr}[f(r,a',R)] + \left(\frac{\hbar}{m_\pi c}\right)^2 \frac{1}{r} V_s(\vec{\sigma}\cdot\vec{l})\frac{d}{dr}[f(r,a,R_0)] + V_{\text{Coul}} .$$

The form factor f was $f(r,a,R) = \{1 + \exp[(r-R)/a]\}^{-1}$, with $R = R_0[1 + \sum_{\lambda\mu}\alpha_{\lambda\mu}Y_{\lambda\mu}(\theta,\phi)]$ for vibrational nuclei and $R = R_0[1 + \sum_{\lambda'}\beta_{\lambda'}Y_{\lambda'0}(\theta')]$ for rotational nuclei, with notation as defined in Ref. 13. The spin-orbit potential was not deformed and thus did not contribute to the coupling. The depths of the real and imaginary potentials were given by $V = V_0 \pm V_1(N-Z)/A + \Delta_c$, $W_V = W_{V0}$, and $W_D = W_{D0} \pm W_1(N-Z)/A$, where the notation for the isospin terms is that of Satchler[34] and Δ_c is the Coulomb correction term.[34]

Numerical calculations were carried out using a modified version of the code **JUPITOR 1** by Tamura.[13] Only coupling between the ground state (0^+) and first excited state (2^+) was considered; i.e., only quadrupole deformations were considered in the present study. The second excited states for these nuclei have spins and parities either 3^- or 4^+; therefore, we have chosen the simplest and most coherent coupling basis in the target spin state, i.e., $0^+, 2^+$. Complex coupling was employed throughout for this work.

The Sm data were fitted first. For the Sm isotopes the magnitudes of the potential strengths were, in MeV: $V_0 = 49.82 - 0.22E$; $V_1 = 18$; $\Delta_c = 0.3\ Z/A^{1/3}$ for incident protons and $\Delta_c = 0$ for incident neutrons; $W_{V0} = -1.28 + 0.16E$ or 0, whichever is greater; $W_{D0} = 4.06 + 1.1\sqrt{E}$ for $E \leq 8$ MeV and $W_{D0} = 7.17 - 0.05E$ for $E > 8$ MeV; $W_1 = 9$; and $V_s = 8.5$. The choice $W_1/V_1 = \frac{1}{2}$ was based on the work of Becchetti and Greenlees.[42] The geometric parameters, in fm, were $R_0 = 1.25A^{1/3}$, $a = 0.65$, and $a' = 0.58$. The strength and energy variation of the real potential have slightly different values from those already published[9] but give essentially the same σ_T values at $E_n = 7$ MeV. The strength and energy variation of the absorptive surface potential (W_D) was changed in order to fit the experimental inelastic scattering results[38] at $E_n = 4.08$ MeV and to obtain the same values previously reported[9] at $E_n = 7$ MeV.

Since the potential given above for Sm gave good fits to the Sm data (see, e.g., Figs. 2, 5, 6), it was decided, following Glendenning *et al.*,[3] to fit the Nd data with only small adjustments to the strength parameters of this potential. (In principle, no changes are necessary because of the presence of the isospin terms.) Only the strength

TABLE II. Comparison of experimental values of low-energy neutron scattering parameters with calculated values at 10 keV for Nd.

	^{142}Nd		^{144}Nd		^{146}Nd		^{148}Nd		^{150}Nd	
Parameter	Exp.	Calc. $\beta_2 = 0.09$	Exp.	Calc. $\beta_2 = 0.12$	Exp.	Calc $\beta_2 = 0.15$	Exp.	Calc. $\beta_2 = 0.18$	Exp.	Calc. $\beta_2 = 0.21$
$S_0(\times 10^4)$	1.4 ± 0.4[a]	2.25	3.9 ± 1.0[a]	2.85	2.3 ± 0.6[a]	3.77	3.0 ± 0.6[a]	5.16 (Rot.) 5.04 (Vib.)	3.2 ± 0.6[a]	2.77
$S_1(\times 10^4)$[b]	1.0 ± 0.4[c]	1.61	0.8 ± 0.8[d]	1.73	0.8 ± 0.8[d]	1.98	0.8 ± 0.8[d]	1.67 (Rot.) 2.32 (Vib.)		1.80
R'(fm)		4.40	7.6 ± 3.0[d]	4.42	8.7 ± 3.4[d]	4.75	8.2 ± 3.1[d]	8.12 (Rot.) 5.71 (Vib.)		8.15

[a] Reference 35.
[b] We assumed $a_c = 1.25A^{1/3}$ for the channel radius.
[c] Reference 36.
[d] Reference 19.

TABLE III. Comparison of experimental values of low-energy neutron scattering parameters with calculated values at 10 keV for Sm.

	^{148}Sm		^{150}Sm		^{152}Sm		^{154}Sm
Parameter	Calc. $\beta_2=0.13$	Exp.	Calc. $\beta_2=0.17$	Exp.	Calc. $\beta_2=0.22$	Exp.	Calc. $\beta_2=0.24$
$S_0(\times10^4)$	3.62	3.6 ± 0.3[a]	5.65 (Rot.) 5.58 (Vib.)	2.2 ± 0.4[a]	2.00	1.8 ± 0.5[a]	1.37
$S_1(\times10^4)$[b]	1.43		1.30 (Rot.) 1.84 (Vib.)	0.9 ± 0.9[c]	1.56	$3.0(+1.3-0.7)$[d]	1.62
R'(fm)	4.21		8.32 (Rot.) 5.61 (Vib.)	8.2 ± 0.7[a]	8.16	8.2 ± 0.7[a]	7.82

[a] Reference 35.
[b] We assumed $a_c=1.25A^{1/3}$ for the channel radius.
[c] Reference 19.
[d] Reference 37.

parameters V_0 and W_{D0} were adjusted. For Nd, the values of these parameters were, in MeV: $V_0=50.2-0.22E$; and $W_{D0}=4.7+1.1\sqrt{E}$ for $E\leq8$ MeV and $W_{D0}=7.81-0.05E$ for $E>8$ MeV. The remaining Nd parameters were the same as those for Sm.

The comparison between calculated and measured neutron scattering parameters at very low energies is presented in Table II for the Nd isotopes and Table III for the Sm isotopes. These parameters include the s-wave strength function (S_0), the p-wave strength function (S_1), and the potential scattering radius (R'), all of which are defined in Ref. 35. For the transitional nuclei ^{148}Nd and ^{150}Sm, both rotational model and vibrational model calculations are presented. We note here that S_1 and R' appear more sensitive to the choice of model than S_0. Unfortunately, no data on S_1 and R' exist at present for ^{150}Nd, ^{148}Sm, or ^{150}Sm. It is seen that in several instances, e.g., S_0 for ^{148}Nd in Table II, the discrepancy between experimental values and calculated values is large. Nevertheless, in view of the large uncertainties associated with the experimental values of these parameters, it is believed that the overall agreement is satisfactory for both elements.

IV. RESULTS

The measured neutron total cross sections for ^{144}Nd and ^{148}Sm are presented in Fig. 2. The error bars indicate statistical uncertainties only, in this figure and all those which follow. The smooth curves are the results of coupled-channel calculations performed using the values of the optical potential parameters given in Sec. III. Both isotopes were assumed to be vibrational nuclei with β_2 values of 0.12 and 0.13 for ^{144}Nd and ^{148}Sm, respectively.

The measured total cross section differences for the Nd isotopes are given in Figs. 3 and 4. We use the convention (larger A – smaller A) for the order of terms in the difference. The data are presented as relative differences; i.e., at each neutron energy the measured difference has been divided by the measured ^{144}Nd total cross section

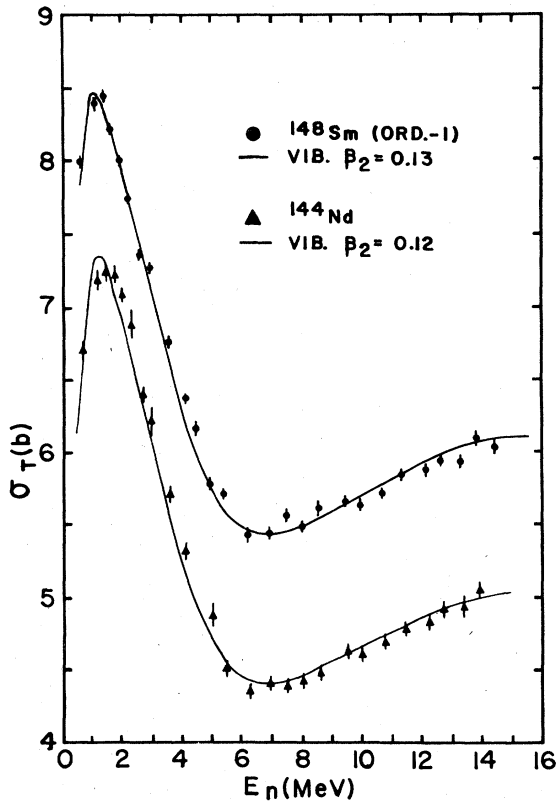

FIG. 2. Total cross sections of ^{144}Nd and ^{148}Sm for neutrons. Error bars indicate statistical uncertainties only, in this figure and all which follow. The curves were calculated using a coupled-channel optical model. See text for details.

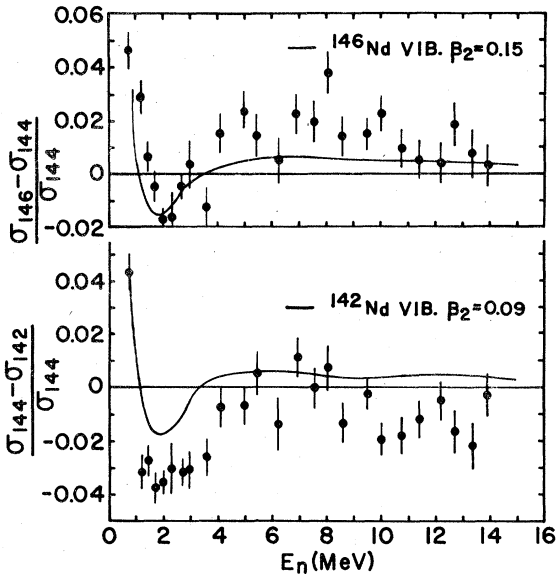

FIG. 3. The measured total cross section difference divided by the ^{144}Nd total cross section for ^{144,142}Nd and ^{146,144}Nd. The curves in this figure and all which follow are results of coupled-channel calculations. The β_2 value employed for ^{144}Nd was the same as that of Fig. 2. See text for details.

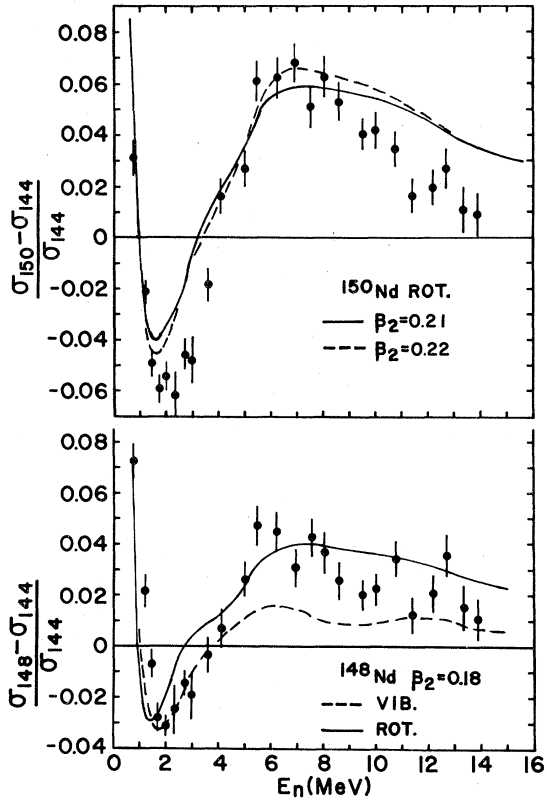

FIG. 4. Relative total cross section differences for ^{148,144}Nd and ^{150,144}Nd. For the former, calculated curves are presented for which ^{148}Nd is assumed either a vibrational nucleus (dashed) or a rotational nucleus (solid). For the latter difference, curves for two values of the ^{150}Nd β_2 parameter are given.

shown in Fig. 2. The errors appear large in Figs. 3 and 4; however, it should be pointed out that determining a relative difference to an uncertainty of 0.01, for example, is equivalent to measuring each of the individual cross sections to a precision of 0.7%. Also shown are relative differences computed using the values of the optical potential parameters given in Sec. III. For ^{144}Nd, the assumptions regarding the type of collective motion and the value of β_2 were those given in Fig. 2. For the other Nd isotopes, these assumptions are given on the figures.

The measured relative differences for ^{150,148}Sm, ^{152,148}Sm, and ^{154,148}Sm are presented in Figs. 5 and 6. Again, the curves were calculated using the parameter values of Sec. III and the assumptions regarding the collective behavior and β_2 value of each isotope are those of Fig. 2 for ^{148}Sm and given on the figures for the remaining nuclei.

The ^{150,148}Sm difference data presented in Fig. 5 show the effect of adding two neutrons to ^{148}Sm. In order to also show the effects of adding two neutrons to ^{150}Sm and ^{152}Sm, the relative differences for ^{152,150}Sm and ^{154,152}Sm were determined by subtracting measured differences. These results and the corresponding calculated curves are given in Fig. 5.

The calculated curves given in Fig. 7 show the sensitivity of the ^{154,148}Sm relative difference to the potential parameters V_1 (top) and β_2 (bottom). For each of these calculated curves, the strength and the geometry of the optical potential for ^{148}Sm were identical to those employed for Fig. 2. Thus, when V_1 was changed (top), an equivalent change was made in V_0 such that, for ^{148}Sm, the value of V at each energy remained the same (see Sec. III). The solid curves in this figure are identical to the solid curve for ^{154,148}Sm in Fig. 6.

The good consistency between the Nd and Sm measurements (see Sec. IIC) suggests that comparisons from element to element are meaningful. The differences (^{148}Sm – ^{146}Nd), (^{150}Sm – ^{148}Nd), and (^{152}Sm – ^{150}Nd) have been computed from the data to show the effects of adding two protons to ^{146}Nd, ^{148}Nd, and ^{150}Nd, respectively. Such a comparison is particularly interesting for these nuclei because for each of the pairs chosen the two members are believed to have very similar deformations.[43] These results, along with the corresponding coupled-channel calculations, are presented as relative differences in Fig. 8.

The sources of error in the determination of

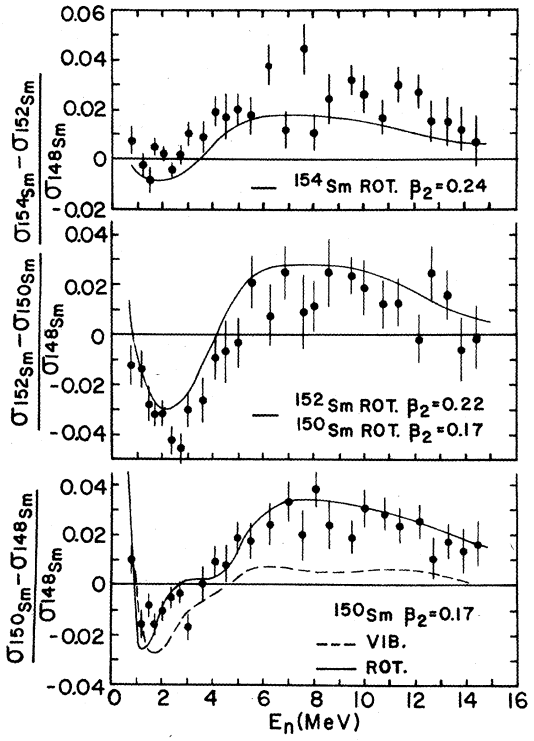

FIG. 5. The measured total cross section difference divided by the ^{148}Sm total cross section for ^{150,148}Sm (bottom). Curves for which ^{150}Sm is assumed vibrational (dashed) and rotational (solid) are given. The β_2 value employed for ^{148}Sm was the same as that of Fig. 2. Also shown are relative differences for ^{152,150}Sm and for ^{154,152}Sm which were computed by subtracting measured differences. This figure shows the effect of adding two neutrons to ^{148}Sm, ^{150}Sm, and ^{152}Sm.

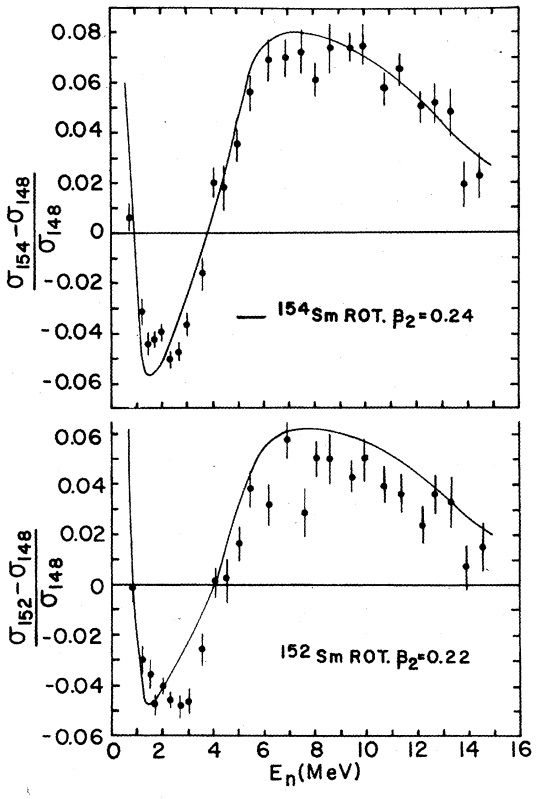

FIG. 6. Relative differences for ^{152,148}Sm and ^{154,148}Sm.

the ^{144}Nd and ^{148}Sm total cross sections can be grouped into two categories: those associated with the samples and those related to measuring the transmissions. The largest of the former category are uncertainties due to impurities in the $^{144}Nd_2O_3$ or $^{148}SmO_3$, including adsorbed water, and in the Be and BeO. The effect of all impurities on each of the total cross section values is estimated to be less than 0.6%. The largest contributors of the latter category are room-scattered background and count rate effects, each of which has an associated cross section error of 0.4% or less. The total systematic uncertainty of each cross section datum is estimated to be about 1% or less. This estimate is consistent with the checks discussed in Sec. II C.

Many of the systematic errors are substantially smaller for the difference measurements than for the total cross section measurements because all the rare earth samples were very similar, both chemically and physically. Since the transmissions were almost equal, transmission-related sources or error such as count rate effects and backgrounds were negligible. And since each of the rare earth oxides contained essentially the same metallic impurities, this source or error also was small. Adsorbed water and inscattering were the largest sources of error, each contributing about 0.003 or less to the uncertainty in the relative difference data except those for ^{142}Nd. For ^{142}Nd, the water contribution ranged from about 0.012 at 0.75 MeV to 0.004 at 14 MeV. The overall systematic error in the relative differences is believed to be about 0.005 or less for all data except ^{142}Nd data, for which it is estimated to range from about 0.01 at low energies to about 0.005 at high energies.

V. DISCUSSION

At low energies the present total cross section data for ^{144}Nd, ^{146}Nd, ^{148}Nd, and ^{152}Sm appear to be consistent with the data of Pineo *et al.*, which extends up to 650 keV.[19] At high energies, the present results can be compared with the data of Dyumin *et al.* at 14.2 MeV.[20] For both Nd and Sm the agreement at 14.2 MeV is very good for the lightest isotope, ^{142}Nd and ^{148}Sm, respectively, but becomes poorer with increasing neutron num-

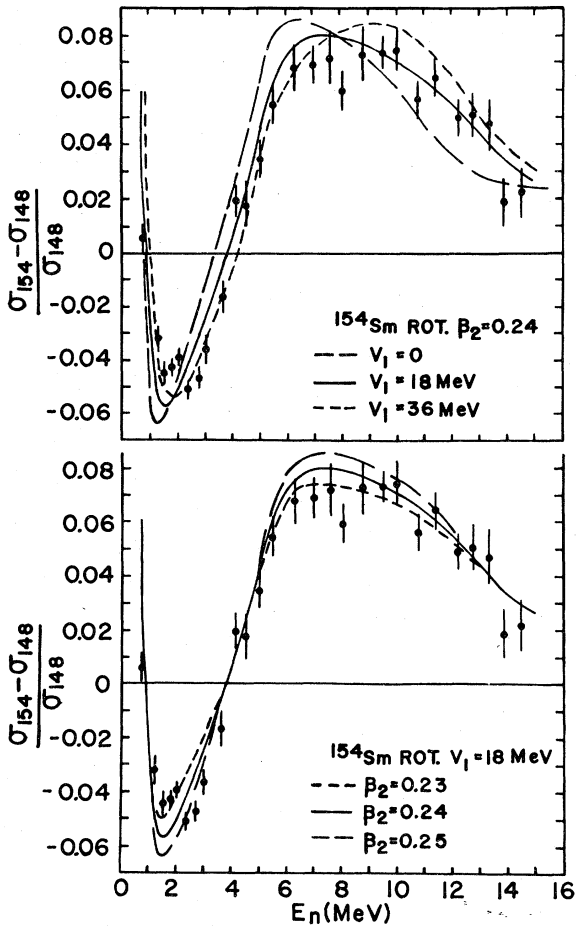

FIG. 7. Effect on the calculated relative difference for ^{154},^{148}Sm of varying the isospin parameter V_1 (top) and the ^{154}Sm deformation parameter β_2 (bottom). Values of all parameters for the ^{148}Sm potential were the same as those in Fig. 2.

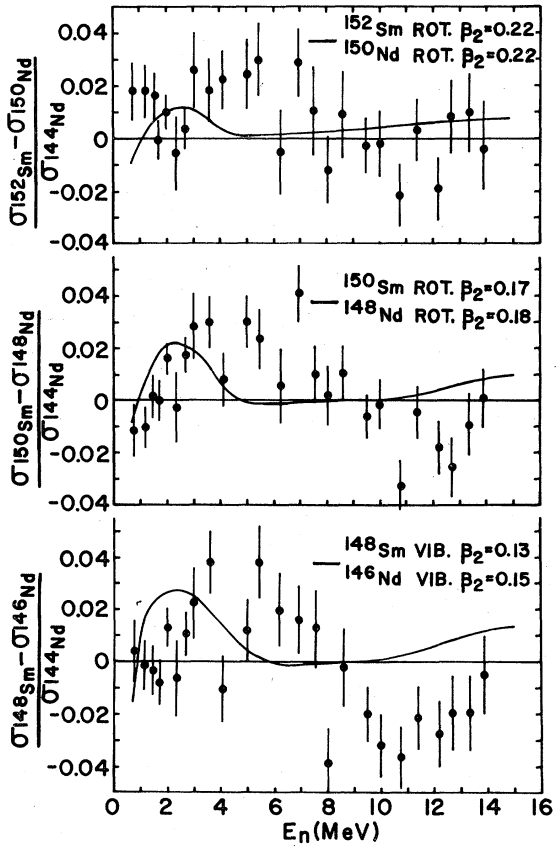

FIG. 8. Effect of adding a proton pair to ^{146}Nd, ^{148}Nd, and ^{150}Nd. The closed circles represent values determined from measured differences.

ber. The data appear to be consistent within experimental uncertainties for Nd, but not for Sm. For the relative difference (^{154}Sm – ^{148}Sm)/^{148}Sm, the worst case, their value[20] would be about 0.11 ± 0.015 (our estimate) as compared to our interpolated value of 0.021 ± 0.011 (see Fig. 6). The discrepancy is almost as large for the ^{152},^{148}Sm relative difference. In view of the excellent agreement between the two experiments for ^{148}Sm, for which nucleus the two measured values were essentially identical, these large variances for ^{152}Sm and ^{154}Sm are difficult to understand.

It is observed that the relative difference data in Figs. 3–6 are characterized by a minimum near 2 MeV and a broad maximum near 7 MeV. It has been pointed out previously in connection with work on the isotopes ^{150},^{152},^{154}Sm that these characteristics are inconsistent with a spherical potential interpretation of the data.[7] This model failed even when allowances were made for the increased diffuseness which might be associated with the surface of a vibrating or rotating nucleus.[7] However, the calculated curves presented in Fig. 7 indicate that a deformed potential model can describe this oscillatory behavior to a high degree of precision. The various calculated curves given in Figs. 3–6 suggest that for this mass region, the observed behavior is a general feature of the total cross section difference (more deformed – less deformed), independent of the type of collective motion assumed. Thus, the data in Figs. 3 and 4 and Figs. 5 and 6 indicate that the addition of neutron pairs to ^{142}Nd and ^{148}Sm increases the nuclear potential deformation of the Nd isotopes and the Sm isotopes, respectively. This observation is consistent with measurements of these nuclei which are sensitive only to the proton distribution.[43]

The oscillatory behavior of the relative differences shown in Fig. 3–6 is similar in character to the variation with energy of $\Delta\sigma_{def}$, the nuclear deformation effect of oriented targets. We believe that the present results have the same qualitative

explanation.[10,18,44] It is well known that the broad maxima observed in neutron total cross sections such as those near 1.5 MeV in Fig. 2 are a consequence of the nuclear Ramsauer effect, that is, the destructive interference between the part of the neutron wave going around the nucleus with the portion going through it.[45] It is also known that in this mass region the maxima move to higher energies with increasing nuclear radius.[46] For neutrons incident on an ensemble of spherical nuclei, for example, each neutron wave will have the same path length through nuclear matter; consequently, these maxima will be relatively sharp. However, for neutrons incident on either rigidly deformed or vibrating nuclei, the path lengths will differ, thus spreading the peaks and filling the valleys of the total cross section curve. This simple model predicts that for the present data (see Fig. 2), the relative difference [(deformed – spherical)/spherical] should be negative near 1.5 MeV and positive near 7 MeV, as is indeed observed in Figs. 3–6.

It is noted in Figs. 3 and 4 that the maximum in the Nd data near 7 MeV increases in magnitude with an increase in the A difference between the two isotopes. This effect can be explained quantitatively for these data in terms of partial cross sections. Haouat *et al.* have measured, at 7 MeV, differential cross sections for neutron scattering from these same Nd isotopes.[39] The integrated *elastic* cross section was found to remain essentially constant from isotope to isotope. The integrated *inelastic* cross sections increased with A quantitatively in agreement[39] with the 7 MeV data shown in Figs. 3 and 4. Thus, this increase in the relative difference maximum with A can be attributed primarily to increased inelastic scattering.

It was surmised in earlier experimental work on ^{150,152,154}Sm that δ, the change in the relative difference between the 7 MeV maximum and the 2 MeV minimum (e.g., about 0.12 for ^{148,154}Sm in Fig. 6), is a measure of the difference in deformation between these two isotopes.[7] The calculated curves given in Fig. 7 (bottom) support this earlier conjecture.

The data presented in Fig. 5 show the effect of adding two neutrons to ^{148}Sm, ^{150}Sm, and ^{152}Sm. It is observed that in each case the deformation increases. In addition, the large value of δ for ^{152,150}Sm as compared to ^{154,152}Sm, for example, indicates that adding a pair of neutrons to ^{150}Sm increases the nuclear deformation more than adding a pair to ^{152}Sm. It is noted that this interpretation is supported quantitatively by the coupled channel calculations.

The data of Fig. 8 indicate that the effect of adding a proton pair to nuclei in this mass range is quite different than adding a neutron pair. It is observed that these relative differences are positive at low energies and near zero or negative at high energies, i.e., essentially a reversal of the effect observed in Fig. 5. In Fig. 8, the calculations and data for (^{152}Sm – ^{150}Nd), whose nuclei are believed to have very smiliar deformation properties, suggest that part of this effect is a consequence of the difference in radius (or potential strength, because of the VR^n ambiguity). Obviously this "reversed" deformation effect can occur, also, if the order of terms in the relative difference is (less deformed – more deformed), i.e., the converse of the order in Fig. 5. The somewhat enhanced effect observed in Fig. 8 for the (^{148}Sm – ^{146}Nd) difference appear to arise from this cause. Thus, unlike the case for neutrons, adding a proton pair to nuclei in this mass region appears either to leave the nuclear deformation unchanged or to decrease it slightly. This result seems to be consistent with data on the proton distribution of these nuclei.[43]

It is seen in Figs. 2 and 7 that the deformed potential model of the present work provides excellent fits to the ^{148}Sm total cross sections and ^{154,148}Sm relative differences for very reasonable potential parameters. For $V_1 \simeq 25$ MeV and a β_2 of 0.24 for ^{154}Sm, for example, it is seen that the present model would fit both the ^{148}Sm and ^{154}Sm total cross sections to about 1% from 0.75 to 14.5 MeV. Only the n-p total cross section has a better fit with a physically meaningful model over this neutron energy range.[31] This good agreement probably is a consequence of the fact that the collective properties of these nuclei are consistent with the model employed; i.e., ^{148}Sm and ^{154}Sm are good examples of vibrational nuclei and rotational nuclei, respectively.[12]

It is seen in Fig. 5 that calculations which assume that ^{150}Sm is a rigid rotator fit the measured ^{150,148}Sm relative differences significantly better than those which assume that ^{150}Sm is a vibrational nucleus. The vibrational fit cannot be improved appreciably by increasing β_2 to improve the higher energy fit, since the fit to the low energy data then becomes worse. Since there is experimental[47] and theoretical[5] evidence that ^{150}Sm is neither a pure rotator or vibrator, this good agreement with a rotator description is unexpected. Recent static and dynamic Hartree-Fock-Bogoliubov (HFB) calculations indicate that ^{150}Sm is a soft, weakly deformed nucleus.[5]

It is observed in Fig. 6 that the present deformed potential model does not fit the ^{152,148}Sm relative difference as well as that for ^{154,148}Sm, particularly near 3 MeV. Changing β_2 and V_1 does

not improve the overall fit significantly, as can be deduced from Fig. 7. The obvious explanation for this discrepancy is that the type of collective motion assumed for ^{152}Sm is not correct, i.e., that ^{152}Sm is not a pure rotator. The vibrational and rotational calculated curves for ^{150,148}Sm presented in Fig. 5 suggest that similar curves for ^{152,148}Sm would bracket the data of Fig. 6; in other words, these data suggest that ^{152}Sm also undergoes vibrational motion. Recent $(n,n'\gamma)$ studies[48] on ^{152}Sm and theoretical work[49] on ^{152}Sm and ^{154}Gd (expected to have collective properties similar to ^{152}Sm) support this explanation.

Figure 7 (top) shows the effect of the real isospin term (or asymmetry term) of the optical potential on total cross section differences. Evidence that such a term is necessary to fit neutron total cross section data was first reported by the Leningrad group in connection with measurements at 14.2 MeV on several chains of isotopes.[50] The sensitivity of total cross section *difference* measurements to this term has been pointed out previously by Shamu *et al.*[21] The calculated curves given here show that in the present work the main effect of the real isospin term of the optical potential is to shift the zero crossover near 4 MeV of the total cross section difference curve. This effect is of interest since this crossover is relatively insensitive to changes in β_2, as shown in the bottom part of Fig. 7. Thus, at least for the nuclei considered herein, isospin effects and deformation effects do not appear to be strongly interdependent for calculations of total cross section differences. These results strongly suggest that total cross section difference measurements may yield accurate values for the isospin parameters of the nuclear optical potential.[21]

The calculated curves presented in Fig.7 (bottom) show that the dependence of the relative difference on δ, the maximum minus minimum of the oscillation, is large. It is observed that a change in β_2 of 4% causes δ to change by 8%, i.e., $\delta \simeq (\beta_2)^2$. This dependence is similar to that of the inelastic scattering cross section to the 2^+ state.[13] It is noted in Fig. 7 (top) that the value of δ does not depend significantly on V_1 for reasonable values of this parameter, 18 to 36 MeV. Thus, the data and calculations presented in Fig. 7 suggest that the value of β_2, the quadrupole deformation of the nuclear potential, may be determined to good precision from measurements such as those of the present work.[21]

As mentioned in Sec. III, the optical potential employed for the Nd calculations was almost identical to the potential obtained by fitting the Sm data except, of course, for variations in β_2. The only changes made for Nd were minor adjustments to the strength parameters V_0 and W_{D0}. Figures 2–6 show that this procedure is not adequate for this total cross section data in that the resulting fits generally are poor for Nd in comparison to those for Sm. In Fig. 2, for example, it is seen that the ^{144}Nd fit is not as good as the Sm fit from 1 to 5 MeV. This discrepancy probably contributes to the poor quality of the fits over the same energy range for the Nd relative differences shown in Fig. 3 and 4. The fit for the ^{144,142}Nd difference is especially poor; however, this problem may be due in part to water adsorbed by the ^{142}Nd sample. In this case the agreement could be improved substantially by raising the data points an amount ranging from 0.01 at low energies to 0.005 at high energies, which for these data is consistent with the systematic error caused by adsorbed water (see Sec. IV). No disparity between the Nd and Sm fits is observed for the differential cross section data at 4 MeV (Ref. 38) and 7 MeV,[9,39] probably because at those particular energies the total cross section fits are reasonable for both elements.

Within the constraints of the present model (see Sec. III), an adjustment of the optical model parameters to fit the Nd total cross section data tends to worsen agreement with the Sm data. Clearly this is the case for the data of Fig. 2, for example. Here, since ^{144}Nd and ^{148}Sm have essentially the same value of $(N-Z)/A$, modifying V_1 in order to shift the ^{144}Nd calculated curve would shift the ^{148}Sm curve by about the same amount. Thus, the present model must be altered if one wishes to fit precisely all the data of Figs. 2–6. The modifications which are required will be the subject of a future report.

The data presented in Figs. 5 and 8 show that, in this mass region, neutron total cross sections change in a systematic way when either two neutrons or two protons are added to a nucleus. This behavior probably is a consequence of regular changes in size and/or deformation with neutron or proton number and strongly suggests the possibility of determining unknown neutron total cross sections with reasonable precision simply by the method of extrapolation from known ones (provided, of course, that the difference in A is small).

This method has been employed by Moore *et al.*[51] to estimate the neutron total cross section of ^{242}Pu between 0.7 and 20 MeV using measured ^{238}U total cross sections as a base. An extrapolation procedure would be expected to be valid for this mass range since here, just as for Nd and Sm, nuclear quadrupole deformation changes monotonically with neutron number.[52] These authors approximated the effects of the addition of two neutrons and two protons to ^{238}U as the difference

TABLE IV. Values of β_2 deduced from the present analysis ($R_0 = 1.25A^{1/3}$ fm).

Element	Mass number 142	144	146	148	150	152	154
Nd	0.09	0.12	0.15	0.18	0.22		
Sm				0.13	0.17	0.22	0.24

in measured total cross sections between ^{239}Pu and ^{235}U; i.e., the assumption made was

$$\sigma_T(^{242}\mathrm{Pu}) = \sigma_T(^{238}\mathrm{U}) + [\sigma_T(^{239}\mathrm{Pu}) - \sigma_T(^{235}\mathrm{U})].$$

(The presence of the odd neutron in each of the odd-A nuclei is unimportant since, in the energy range of interest, total cross sections depend strongly only on the *collective* nuclear states.) The estimated total cross sections for ^{242}Pu were found to be in very good agreement with measured values. As Moore *et al.* point out, this method is particularly useful for those nuclei for which total cross section measurements are not possible because, for example, of insufficient amounts of materials.[51]

All of the β_2 values deduced from the present analysis are listed in Table IV. It should be emphasized that the values listed for Sm do not differ substantially from those of a previous analysis based only on total cross section and low-energy data.[21] In other words, the total cross sections presented herein play a significant role in determining these quadrupole parameters. For Sm, some comparisons between these β_2 values and those obtained using other probes have been made already.[9,21] A detailed discussion of β_2 values for all the Nd and Sm isotopes studied in the present work will be given in a later report.[38]

VI. CONCLUSIONS

The present study demonstrates that neutron total cross section measurements offer a simple, but precise, means for studying the deformation of the nuclear potential. For the elements Nd and Sm the relative total cross section difference between even-A isotopes is found to have an oscillatory behavior when plotted as a function of incident neutron energy. This behavior can be explained as a deformation effect *qualitatively* in terms of interference of the incident neutron wave and *quantitatively* with the aid of a coupled-channel optical model. The coupled channel calculations indicate that the peak-to-peak amplitude of the oscillation in the total cross section difference curve, δ, has a strong dependence on β_2; for example, near 4 MeV the dependence is $\delta \simeq (\beta_2)^2$. Neutron measurements on oriented ^{165}Ho nuclei,[10] which have yielded a similar oscillatory behavior, suggest that these oscillations may persist for incident neutron energies as high as 150 MeV. The calculations show also that the difference curve is fairly sensitive to the real isospin term of the optical model. The present work suggests that extending difference measurements to higher energies may define V_1, and possibly W_1, more precisely.

It is observed that adding a neutron pair to each of the isotopes studied has the same qualitative effect on the neutron total cross section. Coupled channel calculations show that the observed effect is consistent with an increase in deformation of the nuclear potential (an increase in deformability for vibrational nuclei). However, adding a proton pair to each of the Nd nuclei, for example, causes an effect which is compatible with *no* increase in potential deformation. These two results are in accord with studies of the nuclear charge distribution.[12] In addition, the fact that neutron total cross sections change in a systematic way when either a neutron pair or proton pair is added suggests that total cross sections which are difficult to measure may be approximated by an extrapolation procedure.

The consequence that precise fits could not be obtained for all the total cross section data indicates that the present model requires some modification. In particular, the presence of only a neutron excess term did not permit sufficient freedom to fit both Nd and Sm data. An additional term, one that depends on Z and/or A, seems to be required.

Finally, the results of coupled-channel optical model analyses performed both with and without differential cross section data demonstrate that neutron total cross section data alone can determine the quadrupole parameter of the nuclear potential to good precision.

Tabulated values of the total cross sections and total cross section differences of the present work are on file at the National Nuclear Data Center, Brookhaven National Laboratory, Upton, New York, 11973.

ACKNOWLEDGMENTS

It is a pleasure to thank Isotope Sales, Oak Ridge National Laboratory, for the loan of the enriched isotopes and the Western Michigan University Faculty Research Fund for financial assistance with the Nd loan. We are also grateful to Kalamazoo Radiology for x-raying the carbon and polyethylene samples. Among the individuals who have contributed to this work, we are particularly indebted to H. Gwinn for advice on drying the samples, T. Tamura and C. Y. Wong for help and advice in the early states of this project, G. Gogny for

several helpful discussions about the properties of the Sm isotopes, A. Michaudon for support and encouragement during visits by one of us (R.E.S.) to Bruyères-le-Châtel, and M. Soga for the proof given in the Appendix.

APPENDIX

It is straightforward to show that the neutron total cross section depends on the deformation only of the ground state of the target nucleus by use of the closure property.[11]

The matrix element for the transition $a \rightarrow b$ can be written

$$M_{ab} = \int \Psi_b^* M \Psi_a \, d\tau \,, \tag{1}$$

where Ψ_a and Ψ_b represent the total wave function of the composite system for the initial state and final state, respectively, and M is an operator causing the transition. The cross section corresponding to the reaction $a \rightarrow b$ is given by

$$\sigma_{ab} = v_a^{-1} |M_{ab}|^2 \,, \tag{2}$$

and the total cross section by

$$\sigma_a = \sum_b \sigma_{ab} \,, \tag{3}$$

where the summation is over all final states, including the initial state a. When (1) and (2) are substituted into (3), one obtains

$$\sigma_a = v_a^{-1} \int\int \Psi_a^*(\tau) M^\dagger \left[\sum_b \Psi_b(\tau) \Psi_b^*(\tau') \right] M \Psi_a(\tau') \, d\tau \, d\tau' \,,$$

where $M^\dagger$ is the adjoint of M. Because of the closure property, the sum in square brackets equals $\delta(\tau - \tau')$. Thus we have

$$\sigma_a = v_a^{-1} \int \Psi_a^*(\tau) |M|^2 \Psi_a(\tau) \, d\tau \,,$$

which depends only on the initial state of the composite system. In the present work this initial state consists of the incident neutron and the ground state of the target nucleus.

---

*Present address: Sandia National Laboratory, Albuquerque, New Mexico 87185.

[1]R. C. Barrett and D. F. Jackson, *Nuclear Sizes and Structure* (Clarendon, Oxford, 1977).
[2]W. Bertozzi, J. Phys. Soc. Jpn. Suppl. 44, 173 (1978).
[3]D. L. Hendrie, N. K. Glendenning, B. G. Harvey, O. N. Jarvis, H. H. Duhm, J. Saudinos, and J. Mahoney, Phys. Lett. 26B, 127 (1968); N. K. Glendenning, D. L. Hendrie, and O. N. Jarvis, *ibid.* 26B, 131 (1968).
[4]G. R. Satchler and W. G. Love, Nucl. Phys. A172, 449 (1971); G. R. Satchler, Phys. Lett. 39B, 495 (1972).
[5]D. Gogny, in *Proceedings of the International Conference on Nuclear Self-Consistent Fields, Trieste, 1975*, edited by G. Ripka and M. Porneuf (North-Holland, Amsterdam, 1975), p. 333; M. Girod, K. Kumar, B. Grammaticos, and P. Aguer, Phys. Rev. Lett. 41, 1765 (1978).
[6]D. M. Chase, L. Wilets, and A. R. Edmonds, Phys. Rev. 110, 1080 (1958).
[7]R. E. Shamu, E. M. Bernstein, D. Blondin, J. J. Ramirez, and G. Rochau, Bull. Am. Phys. Soc. 17, 901 (1972); R. E. Shamu, E. M. Bernstein, D. Blondon, J. J. Ramirez, and G. Rochau, Phys. Lett. 45B, 241 (1973).
[8]Ch. Lagrange, R. E. Shamu, T. Burrows, G. P. Glasgow, G. Hardie, and F. D. McDaniel, Phys. Lett. 58B, 293 (1975).
[9]M. T. McEllistrem, R. E. Shamu, J. Lachkar, G. Haouat, Ch. Lagrange, Y. Patin, J. Sigaud, and F. Cocu, Phys. Rev. C 15, 927 (1977).
[10]H. Marshak, A. Langsford, T. Tamura, and C. Y. Wong, Phys. Rev. C 2, 1862 (1970).
[11]M. Soga (private communication).
[12]A. Bohr and B. R. Mottelson, *Nuclear Structure* (Benjamin, Reading, Mass., 1975), Vol. 2.
[13]T. Tamura, Rev. Mod. Phys. 37, 679 (1965).
[14]Ch. Lagrange and N. Mondon, internal report, Centres d'Etudes de Limeil, France, 1973 (unpublished); Ch. Lagrange, J. Phys. (Paris) Lett. 35, 111 (1974).
[15]J. P. Delaroche, Ch. Lagrange, and J. Salvy, IAEA Report No. IAEA-190, 1976, Vol. II, p. 251 (unpublished).
[16]R. Wagner, P. D. Miller, T. Tamura, and H. Marshak, Phys. Rev. 139, B29 (1965).
[17]D. W. Glasgow and D. G. Foster, Phys. Rev. C 3, 604 (1971).
[18]C. Y. Wong, T. Tamura, H. Marshak, and A. Langsford, Part. Nucl. 4, 163 (1972).
[19]W. Pineo, M. Divadeenam, E. G. Bilpuch, K. Seth, and H. W. Newson, Ann. Phys. (N.Y.) 84, 165 (1974); W. Pineo, Ph.D. dissertation, Duke University, 1970 (unpublished).
[20]A. N. Dyumin, A. I. Egorov, G. N. Popova, and V. A. Smolin, Izv. Akad. Nauk SSSR Ser. Fiz. 37, 1019 (1973) [Bull. Acad. Sci. USSR Phys. Ser. 37, No. 5 (1973)].
[21]R. E. Shamu, E. M. Bernstein, and J. J. Ramirez, Bull. Am. Phys. Soc. 19, 103 (1974); R. E. Shamu, G. Haouat, J. Lachkar, Ch. Lagrange, M. McEllistrem, Y. Patin, J. Sigaud, F. Cocu, E. M. Bernstein, and J. J. Ramirez, National Soviet Conference on Neutron Physics, Kiev, USSR, 1975 [Neutron Phys. 4, 237 (1976)]; R. E. Shamu, Ch. Lagrange, E. M. Bernstein, J. J. Ramirez, T. Tamura, and C. Y. Wong, Phys. Lett. 61B, 29 (1976).
[22]R. E. Shamu, E. M. Bernstein, and Ch. Lagrange, Bull. Am. Phys. Soc. 20, 1196 (1975).
[23]The isotopically enriched Nd_2O_3 and Sm_2O_3 oxides

were obtained on loan from the Research Materials Collection, Isotope Sales Center, Oak Ridge National Laboratory, Oak Ridge, Tennessee.
[24]Supplied by Ventron Corp., Beverly, Massachusetts.
[25]Supplied by Kawecki Berylco Industries, Inc., Hazelton, Pennsylvania.
[26]Supplied by the Radiochemical Centre, Amersham, Buckinghamshire, England.
[27]J. C. Davis and H. H. Barschall, Phys. Lett. 27B, 636 (1968).
[28]R. E. Shamu, E. M. Bernstein, and M. J. Parrott, Nucl. Instrum. Methods 114, 605 (1974).
[29]D. W. Miller, *Fast Neutron Physics* (Interscience, New York, 1963), Part II, p. 985.
[30]R. B. Schwartz, R. A. Schrack, and H. T. Heaton II, in *MeV Neutron Total Cross Sections*, NBS Monograph 138 (U.S. GPO, Washington, D.C. 1974).
[31]J. C. Hopkins and G. Breit, Nucl. Data Tables A9, 137 (1971).
[32]J. C. Davis and H. H. Barschall, Phys. Rev. C 3, 1798 (1971).
[33]H. Feshbach, Ann. Phys. (N.Y.) 19, 287 (1962).
[34]G. R. Satchler, in *Isospin in Nuclear Physics*, edited by D. H. Wilkinson (North-Holland, Amsterdam, 1969), p. 389.
[35]*Resonance Parameters*, compiled by S. F. Mughabghab and D. I. Garber, Report No. BNL-325 (National Tech. Inf. Service, Springfield, Va., 1973), 3rd ed., Vol. I.
[36]J. Boldeman (private communication).
[37]L. R. Fawcett, Ph.D. dissertation, Virginia Poly. Inst. and State Univ., 1971 (unpublished).
[38]R. E. Shamu, G. Haouat, J. Lachkar, M. T. McEllistrem, Ch. Lagrange, J. Sigaud, J. P. Delaroche, Y. Patin and F. Cocu, in *Proceedings of the International Conference on the Interactions of Neutrons with Nuclei, Lowell, Mass., 1976*, edited by E. Sheldon, Report No. Conf-760715-P2 (ERDA, Oak Ridge, 1976), p. 1327; R. E. Shamu *et al.*, Phys. Rev. C (to be published).
[39]G. Haouat, J. Lachkar, Ch. Lagrange, M. T. McEllistrem, Y. Patin, R. E. Shamu, and J. Sigaud, Phys. Rev. C 20, 78 (1979).
[40]P. Stoler, M. Slagowitz, W. Makofske, and J. Kruse, Phys. Rev. 155, 1334 (1967).
[41]J. P. Delaroche and Ch. Lagrange, in *Proceedings of the International Conference on the Interactions of Neutrons with Nuclei* (see Ref. 38), p. 1447; Ch. Lagrange *et al.*, Nucl. Phys. (in press).
[42]F. D. Becchetti and G. W. Greenlees, Phys. Rev. 182, 1190 (1969).
[43]P. H. Stelson and L. Grodzins, Nucl. Data A1, 21 (1965).
[44]T. R. Fisher, R. S. Safrata, E. G. Shelley, J. McCarthy, S. M. Austin, and R. C. Barrett, Phys. Rev. 157, 1149 (1967).
[45]J. M. Peterson, Phys. Rev. 125, 955 (1962).
[46]K. W. McVoy, Ann. Phys. (N.Y.) 43, 91 (1967).
[47]D. Cline, P. Jennens, C. W. Towsley, and H. S. Gertzman, J. Phys. Soc. Jpn. Suppl. 34, 443 (1973); L. Grodzins, B. Herskind, D. Somayajulu, and B. Skaali, Phys. Rev. Lett. 30, 453 (1973).
[48]S. P. Sit'ko, E. A. Andreev, and V. K. Basenko, Yad. Fiz. 25, 1119 (1977) [Sov. J. Nucl. Phys. 25, 593 (1977)]; D. F. Coope, S. N. Tripathi, M. C. Schell, J. L. Weil, and M. T. McEllistrem, Phys. Rev. C 16, 2223 (1977).
[49]K. Kumar, Nucl. Phys. A231, 189 (1974); K. Kumar and J. B. Gupta, *ibid.* A304, 295 (1978).
[50]Yu. V. Dukarevich, A. N. Dyumin, and D. M. Kaminker, Nucl. Phys. A92, 433 (1967).
[51]M. Moore, P. Lisowski, G. Morgan, G. Auchampaugh, and R. Shamu, Bull. Am. Phys. Soc. 24, 882 (1979).
[52]C. E. Bemis, F. K. McGowan, J. L. C. Ford, W. T. Milner, P. H. Stelson, and R. L. Robinson, Phys. Rev. C 8, 1466 (1973). Results given in Table II of this paper suggest that hexadecapole deformation effects would cancel for the nuclei of interest here.